Journal of Veterinary Science

JVS

Original Article
Immunology

Check for updates

The changes of immune-related molecules within the ileal mucosa of piglets infected with porcine circovirus type 2

Fengyang Shi [1,†], Qiuming Li [1,†], Zhanming Zou [1,†], Yang Wang [1], Xiaolin Hou [1], Yonghong Zhang [1], Qinye Song [2], Shuanghai Zhou [1,*], Huanrong Li [1,*]

[1]College of Animal Science and Technology, Beijing University of Agriculture, Beijing 102206, China
[2]College of Animal Science and Technology, Hebei Agricultural University, Baoding 071000, China

OPEN ACCESS

*Corresponding authors:
Shuanghai Zhou
College of Animal Science and Technology, Beijing University of Agriculture, No. 7 Beinong Road, Changping District, Beijing 102206, China.
E-mail: shhaizhou@sina.com

Huanrong Li
College of Animal Science and Technology, Beijing University of Agriculture, No. 7 Beinong Road, Changping District, Beijing 102206, China.
E-mail: lihuanrong1@126.com

†Fengyang Shi, Qiuming Li, and Zhanming Zou contributed equally to this work.

ORCID iDs
Fengyang Shi
https://orcid.org/0000-0003-2530-6017
Qiuming Li
https://orcid.org/0000-0003-4828-8149
Zhanming Zou
https://orcid.org/0000-0001-9989-6908

ABSTRACT

Background: Enteritis is one of the most frequently reported symptoms in piglets infected with porcine circovirus type 2 (PCV2), but the immunopathogenesis has not been reported.
Objectives: This study examined the effect of a PCV2 infection on the intestinal mucosal immune function through morphological observations and immune-related molecular detection.
Methods: Morphological changes within the ileum of piglets during a PCV2 infection were observed. The expression of the related-molecules was analyzed using a gene chip. The immunocyte subsets were analyzed by flow cytometry. The secretory immunoglobulin A (SIgA) content was analyzed by enzyme-linked immunosorbent assay.
Results: The PCV2 infection caused ileal villus damage, intestinal epithelial cells exfoliation, and an increase in lymphocytes in the lamina propria at 21 days post-infection. Differentially expressed genes occurred in the defense response, inflammatory response, and the complement and coagulation cascade reactions. Most of them were downregulated significantly at the induction site and upregulated at the effector site. The genes associated with SIgA production were downregulated significantly at the induction site. In contrast, the expression of the Toll-like receptor-related genes was upregulated significantly at the effector site. The frequencies of dendritic cells, B cells, and CD8+T cells were upregulated at the 2 sites. The SIgA content decreased significantly in the ileal mucosa.
Conclusions: PCV2 infections can cause damage to the ileum that is associated with changes in immune-related gene expression, immune-related cell subsets, and SIgA production. These findings elucidated the molecular changes in the ileum after a PCV2 infection from the perspective of intestinal mucosal immunity, which provides insights into a further study for PCV2-induced enteritis.

Keywords: PCV2; immunity; ileum; inflammation; gene chip

INTRODUCTION

Porcine circovirus type (PCV) 2 can infect different organs and induce a range of diseases in piglets [1]. Enteritis, which is characterized by diarrhea, growth retardation, and weight loss, is one of the most common diseases caused by PCV2 [2-4]. The specific morphological

Generated by xmlinkpress

Yang Wang
https://orcid.org/0000-0001-6974-1390
Xiaolin Hou
https://orcid.org/0000-0003-4423-635X
Yonghong Zhang
https://orcid.org/0000-0003-2135-4708
Qinye Song
https://orcid.org/0000-0002-2899-8517
Shuanghai Zhou
https://orcid.org/0000-0002-9551-4332
Huanrong Li
https://orcid.org/0000-0002-0120-0616

Conflict of Interest
The authors declare no conflicts of interest.

Author Contributions
Conceptualization: Li H, Shi F, Zou Z. Data curation: Shi F, Li Q, Zou Z. Formal analysis: Shi F, Zou Z, Hou X, Zhou S, Zhang Y, Song Q. Investigation: Shi F, Li Q, Zou Z, Wang Y. Writing - original draft: Shi F, Li Q, Zou Z. Writing - review & editing: Li H, Shi F, Li Q, Zhou S, Hou X.

changes in enteritis include exfoliation of the intestinal villus, atrophy of small intestinal glands, and lymphocyte infiltration that occurs within the lamina propria, submucosa, and mucous glands of the small intestine [1,5]. In addition, the proliferation of intestinal epithelioid cells and multinucleated giant cells in enteritis could induce granulomas, accompanied by lymphocyte depletion within Peyer's patches [6]. A PCV2 infection can cause obvious inflammation of the small intestinal mucosa and affect the immune function of piglets [2].

The small intestinal mucosa plays a vital role in the mucosal immunity of the body, primarily because more than 50% of the lymphoid tissues are located there, and 80% of the antibodies are produced [7]. The immune system of the small intestinal mucosa is composed mainly of gut-associated lymphoid tissue, which includes induction and effector sites. The induction site is composed of organized tissues, including Peyer's patches and mesenteric lymph nodes on the intestinal wall [8]. The site is responsible for antigen presentation, cytokine secretion, and secretory immunoglobulin A (SIgA) release [9]. The effector site is composed mainly of diffuse lymphoid tissues, including intestinal intraepithelial lymphocytes and lamina propria lymphocytes [8]. This is where cytokines are secreted, and diseased cells are killed [9]. The ileum, where Peyer's patches are mostly located, plays an important role in the intestinal mucosal immunity [10]. PCV2-induced ileal immune functional changes are vital in the study of enteritis caused by PCV2.

This study examined the ileal mucosal changes of piglets after a PCV2 infection to determine the relationship between PCV2 infection, ileal injury, and immune-related molecular changes. In addition, the ileal mucosal immunopathogenic mechanisms caused by PCV2 was examined.

MATERIALS AND METHODS

Animals
Thirty-five-day-old specific-pathogen-free (SPF) large white × landrace piglets were purchased from the Beijing Centre of SPF Swine Breeding and Management, Beijing, China. All piglets were confirmed to be negative for PCV2-specific antibodies by enzyme-linked immunosorbent assay (ELISA; Lvshiyuan Biotechnology Co., Ltd, China) (data not shown). The piglets also tested negative to PCV1, PCV2, porcine parvovirus, porcine pseudorabies virus, classical swine fever virus, and porcine respiratory reproductive syndrome virus by polymerase chain reaction (PCR)/reverse transcription-PCR (RT-PCR) (data not shown).

PCV2 infection
Twelve piglets were divided randomly into the infection and control groups (6 piglets per group). Each piglet of the infection group was inoculated with 5 mL of the first generation of PCV2 SD/2008 strain (GenBank accession number: GQ174519, it was isolated and identified by the Animal Infectious Disease Laboratory of Hebei Agricultural University) with a titer of $10^{5.25}$ TCID$_{50}$/mL by an intramuscular injection. The piglets in the control group were inoculated with virus-free cell culture supernatants. The piglets in the 2 groups were housed in separate rooms with access to food and water *ad libitum*.

Sample collection
Three piglets in each group were euthanized with an overdose of pentobarbital-sodium (80mg/kg; Sinopharm Chemical Reagent Beijing Co., China). Mesenteric lymph nodes and ileal segments were sampled at 21 and 56 days post-infection (dpi) for the morphological

observations and virus detection. The ileal Peyer's patches and surrounding ileal segments were also sampled for gene chip detection and verification. Mesenteric lymph nodes, ileal Peyer's patches (induction site), and approximately 15 cm of the ileal segments (effector site) were harvested for lymphocytes isolation and flow cytometry (FCM).

Histomorphology observation
The ileal segments and mesenteric lymph nodes were made into paraffin sections after fixing, dehydration, transparency, embedding, and sectioning. The paraffin sections were stained by H&E (Solarbio Science & Technology Co., Ltd., China) and observed by optical microscopy (Olympus, Japan).

Gene chip detection of the induction and effector sites
Samples of the induction and effector sites (1 cm^3 per segment) were harvested at 21 dpi. The total RNA was extracted using an RNA extraction kit (Invitrogen, USA) for amplifying and labeling with Cy-3 using a low Input Quick Amp Labeling Kit, One-Color (Agilent Technologies, USA). The labeled complementary RNA (cRNA) was purified using the RNeasy mini kit (QIAGEN, GmBH, Germany). Each array slide was hybridized with 1.65 μg of Cy3-labeled cRNA using the Gene Expression Hybridization kit (Agilent Technologies) in a hybridization oven. The slides were scanned using an Agilent Microarray Scanner (Agilent Technologies), and the data were analyzed using Feature Extraction software 10.7 (Agilent Technologies). The raw data were normalized using the Quantile algorithm for statistical analysis in the Gene Spring Software (Gene Spring).

GX was used to screen for multiple differentially expressed genes. The functions of the differentially expressed genes were analyzed using the bioinformatics resources Database for Annotation, Visualization, and Integrated Discovery (DAVID 6.6; GO). The results of the gene chip are available in the Gene Expression Omnibus (GEO) and were accessible through GEO series accession number GES149144.

A quantitative RT-PCR (qRT-PCR) was used to verify the results of the gene chip. The reaction was performed in triplicate using an SYBR Green Real-time PCR Master Mix (TOYOBO, Japan) in the Mx3005P Detection System (Genetimes, China). The total reaction volume was 20 μL, and it contained the following: SYBR® Green Real-time PCR Master Mix (10 μL), 25 pmol/μL upstream and downstream primers (each for 0.2 μL), template DNA (1.0 μL), and water (8.6 μL). The conditions were as follows: 95℃ for 5 min, followed by 40 cycles of 95℃ for 40 sec, 56℃ for 30 sec, and 72℃ for 30 sec. Water was used to replace the template DNA in the negative control. All results were analyzed using MxPro Software. **Table 1** lists the primer sequences for qRT-PCR.

Isolation of immune cells
The ileal segments were sampled at 21 and 56 dpi. The cells from the mucosa, lamina propria, and Peyer's patches were separated using the method reported elsewhere [11]. The cell viability was detected by trypan blue exclusion. All cells were maintained in RPMI-1640 (phenol red-free) medium supplemented with 10% fetal bovine serum (FBS; Gibco, USA), and the concentration was adjusted to 1×10^6 cells/mL.

Separation of mucosa cells
The ileal segment (10 cm) was sampled aseptically. The Peyer's patches and fat were removed, and the stool in the ileum was washed away with Hank's solution. The ileal

Table 1. Primers used for qRT-PCR and PCR amplification

Genes source/accession No.	Primer sequence (5′-3′)	Annealing temperature/°C	Products/bp
IFNε (NM_001105310)	Forward:5′-CTCTGGATGGTTGGGAGGAA-3′ Reverse:5′-AGCTGCTGTAGTCCTGGTTT-3′	58	198
C1QA (NM_001003924)	Forward:5′-GGACCTCTGCCTGTACATCA-3′ Reverse:5′-CTGAACCCTGGTAAATGCGG-3′	59	185
C5 (NM_001001646)	Forward:5′-TAAGTACACCGCGTCCCTAC-3′ Reverse:5′-CTGGAGGGCTTCTTTACCCA-3′	59	154
CCL25 (NM_001025214)	Forward:5′-GCTATCCATGCTCAAGGTGC-3′ Reverse:5′-CTTCATCCCAAACTGCACCC-3′	59	207
CD163 (NM_213976)	Forward:5′-CGAGTCCCACCTTTCACTCT-3′ Reverse:5′-AGTGAGAGTTGCAGAGGGAC-3′	59	185
IL-1β (NM_001005149)	Forward:5′-TGAATTCGAGTCTGCCCTGT-3′ Reverse:5′-AGTCCCCTTCTGTCAGCTTC-3′	59	194
CCL4 (NM_213779)	Forward:5′-AACCTCTCCTCCAGCAAGAC-3′ Reverse:5′-AGGCTGCTGGTCTCATAGTA-3′	58	191
CCL5 (NM001129946)	Forward:5′-TGAAGATCTCCACAGCTGCA-3′ Reverse:5′-AATACTCCTTCACGTGGGCA-3′	59	153
CXCL9 (NM_001114289)	Forward:5′-GGACGTTGTTCCTGCATCAA-3′ Reverse:5′-GCTGACCTGTTTCTCCCACT-3′	59	198
IL-1α (NM_214029)	Forward:5′-CTACTTCAAATCAGCCGCCc-3′ Reverse:5′-GGCCTGTCAACACTTCACAG-3′	59	158
IL-6 (M80258)	Forward:5′-CTGGCAGAAAACAACCTGAACC-3′ Reverse:5′-TGATTCTCATCAAGCAGGTCTCC-3′	60	94
β-actin (U07786)	Forward:5′-TCATCACCATCGGCAACT-3′ Reverse:5′-TTCCTGATGTCCACGTCGC-3′	59	547
PCV2 (AF381175)	Forward:5′-AGTGAGCGGGAAAATGCAGA-3′ Reverse:5′-TCCTCCGTGGATTGTTCTGT-3′	56	417

qRT-PCR, quantitative reverse transcription-polymerase chain reaction; PCR, polymerase chain reaction.

debris was resuspended successively in a calcium and magnesium-free (CMF)/FBS/ ethylenediaminetetraacetic acid (EDTA) (calcium and magnesium-free phosphate buffer saline supplemented with 10% FBS and 0.02% EDTA) solution and RPMI-1640 medium supplemented with 10% FBS. Cell precipitation was obtained after vortex shocking, incubating, centrifuging, and filtering. Finally, all cells were suspended in RPMI-1640 (phenol red-free) medium supplemented with 10% FBS.

Separation of lamina propria cells

The precipitation of the ileum, which was sampled from the mucosa, was incubated in a CMF/ FBS/EDTA solution. After centrifugation, the precipitate was washed with RPMI-1640 medium supplemented with 10% FBS and Hank's solution supplemented with 5% FBS. The cells were incubated with collagenase while being vortexed, filtered, and centrifuged. Finally, all cells were suspended in RPMI-1640 (phenol red-free) medium supplemented with 10% FBS.

Separation of the Peyer's patch cells

The sampled Peyer's patches were washed with Hank's solution. After removing all fat and connective tissues, the sample was washed with Hank's solution supplemented with 5% FBS and resuspended in a CMF/FBS/Dispase/DNase (CMF/FBS solution supplemented with 150 mg Dispase and 1.5 mg DNase per 100 mL) solution. Cell precipitation was achieved after incubation, filtration, and centrifugation. All cells were suspended in RPMI-1640 (phenol red-free) medium supplemented with 10% FBS.

Flow cytometry and antibodies

Flow cytometry performed in this study included the following: fluorescein isothiocyanate (FITC)-conjugated mouse anti-pig SWC3a monoclonal antibody (74-22-15; Abcam, UK), PE-conjugated mouse anti-pig CD1 monoclonal antibody (76-7-4; Abcam), FITC-conjugated mouse anti-pig SLA CLASS II DR monoclonal antibody (1053H2-18; BD Pharmingen, USA), PE-conjugated CD152(CTLA-4)-muIg (501-050; Ancell, USA), FITC-conjugated mouse anti-pig CD21 monoclonal antibody (4530-02; Southern Biotech, USA), SPRD-conjugated mouse anti-pig CD3 monoclonal antibody (4510-13; Southern Biotech), FITC-conjugated mouse anti-pig CD4 monoclonal antibody (4515-02; Southern Biotech), and PE-conjugated mouse anti-pig CD8 monoclonal antibody (4520-09; Southern Biotech). Goat anti-mouse immunoglobulin (Ig) G1-FITC (ab97239; Abcam), goat anti-mouse IgG1-SPRD (0102-13; Southern Biotech), goat anti-mouse IgG2a-FITC (ab97244; Abcam), goat anti-mouse IgG2a-PE (ab130787; Abcam), goat anti-mouse IgG2b-FITC (STAR134; AbD Serotec, UK), and goat anti-mouse IgG1-PE (278-050; Ancell) were used as the isotype controls.

The intestinal cells from the mucosa, lamina propria, and Peyer's patches were centrifuged separately at 1,500 rpm for 10 min and resuspended in 250 μL of phosphate buffered saline (PBS). Each group of cells was incubated with different types of FCM antibodies. All cells were washed with 1 mL of PBS at 25°C for 30 min to remove the unconjugated antibodies. Each group of cells was centrifuged at 1,500 rpm for 10 min and oscillated in 250 μL of PBS on a vortex oscillator. All samples were analyzed by FCM (EPICS ELITE; Beckman Coulter, USA). The isotype antibody was used as the control. The different cell types were identified as follows: SWC3a$^+$/CD1a$^+$ cells were dendritic cells (DCs); CD21$^+$ cells were B lymphocytes; CD3$^+$ cells were T lymphocytes; CD3$^+$/CD4$^+$/CD8$^-$ cells were helper T cells (Th); CD3$^+$/CD4$^-$/CD8$^+$ cells were cytotoxic CD8$^+$T lymphocytes (CD8$^+$CTL) [12].

T cell proliferation test

The intestinal cells from the mucosa, lamina propria, and Peyer's patches were plated separately into a 96-well plate at an initial concentration of 2×10^5 cells/mL in 200 μL/well in triplicates. ConA (Sigma, USA) was added to the wells of the infected group at a final concentration of 10 μg/mL. RPMI-1640 (phenol red-free) medium was added to the wells of the control group. Plates of the 2 groups were incubated for 72 h. According to the manufacturer's instructions of the MTS Kit (G3580; Promega, USA), 100 μL of the supernatant was discarded, and 20 μL of a mixed solution of MTS and PMS was added to the wells. The optical density (OD) value at 490 nm was measured using a microplate reader (Bio-Tek, USA).

Stimulating index (SI) of lymphocyte proliferation was calculated using the following formula: SI = (OD value of the infection group − OD value of the nutrient solution control group)/(OD value of the unstimulated negative control group − OD value of the nutrient solution control group).

ELISA

The production of SIgA was detected using a SIgA ELISA Kit (E-EL-P1528c; Elabscience, China) according to the manufacturer's instructions. The ileal contents, biotinylated SIgA antibody, and HRP-conjugated avidin were added sequentially to microwells that had been coated with the SIgA antibody. A TMB substrate solution was added for visualization after washing. The OD value was measured at a wavelength of 450 nm using a microplate reader. The concentration of the sample was calculated from the standard curve.

Statistics

The differentially expressed genes were analyzed using DAVID Bioinformatics Resources 6.7 in GO and Pathway software. A t-test was used to assess the other statistical values. The P values were determined, and the error bars represented the standard error of the mean. The *p* values < 0.05 were considered significant and are denoted by *.

Ethical statement

All animal experiments were performed in accordance with the approved protocols from the Beijing University of Agriculture Institutional Animal Care and Usage Committee (approval No. SYXK2016-0007).

RESULTS

PCV2 infection caused ileal damage in piglets

In the preliminary experiment, the infected piglets had a high viral nucleic acid load at 21 days dpi and a lower level at 56 dpi (**Supplementary Fig. 1**). PCR was performed to confirm the presence of PCV2 in the ileum of the infected piglets (**Supplementary Fig. 2**). Compared to the control group at 21 dpi, the villi of the ileum were disrupted severely. The intestinal epithelial cells of ileum were severely detached, and the lymphocytes infiltrated within the lamina propria in the infection group. Moreover, the intraglandular tissues of the ileum were disrupted during the PCV2 infection. The shape and size of the villi were partially restored, but the mucosal tissues were still infiltrated with inflammatory cells in the infection group at 56 dpi (**Fig. 1**). This suggests that the PCV2 infection caused ileal damage to the piglets.
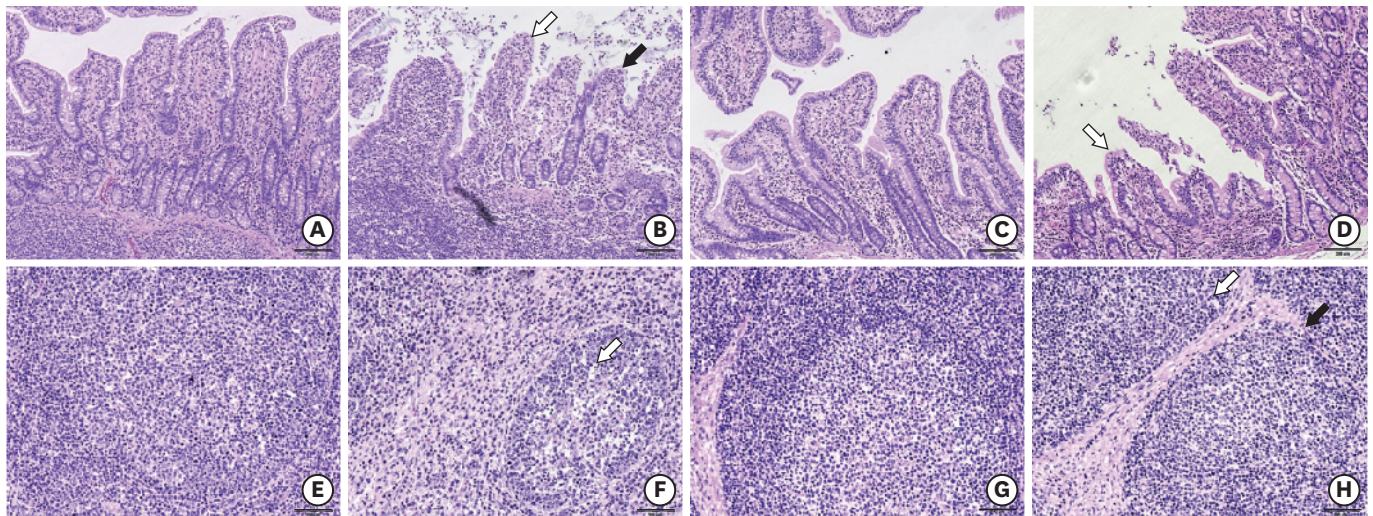
Fig. 1. Morphological changes within the ileum of piglets during PCV2 infection. (A) Histomorphologic observations of the ileum either without PCV2 infection (21 dpi, 100×) or (B) after PCV2 infection (21 dpi, 100×). As indicated by the white arrow, the intestinal epithelial cells of the villus fall off, and the black arrow shows shortening of the villus in the infection group. The mucosal tissues in the infection group were markedly infiltrated with inflammatory cells. (C, D) At 56 dpi, as indicated by the white arrow, the shape and size of the villi were partially restored. On the other hand, the mucosal tissues were still infiltrated with inflammatory cells in the infection group (56 dpi, 100×). (E) The mesenteric lymph nodes of the control group (21 dpi, 200×). (F) The mesenteric lymph nodes of the infected group (21 dpi, 200×). The white arrow indicates that there are fewer lymphocytes. (G) The mesenteric lymph nodes of the control group (56 dpi, 200×). (H) The mesenteric lymph nodes of the infection group (56 dpi, 200×). Scale bar, A-D: 200 μm, E-H: 100 μm.
PCV2, porcine circovirus type 2; dpi, days post-infection.

PCV2 infection inhibited the immune function of the induction site and antiviral capacity of the effector site

The gene expression of the ileum at 21 dpi was analyzed using a gene chip. GO analysis showed that the expression of the genes related to defense responses, inflammatory responses, complement and coagulation cascades reactions, and the production of SIgA were changed at the induction site. Fifteen differentially expressed genes were involved (2 were upregulated, and 13 were downregulated) (**Table 2**). The expression of the genes associated with complement and coagulation-signaling cascades, *C1QA*, *C5*, *C6*, *C8A*, *C9*, *CFH*, and *F5* were downregulated. The expression of anticoagulant molecule 5 was downregulated significantly. Furthermore, the expression of genes related mainly to the inflammatory and defense responses, *C1QA*, *C5*, *SAA2*, and *CD163*, were downregulated. The expression levels of the genes related to the production of *IgA*, *CCL25*, *CCL28*, and *PIGR* were also downregulated. The results suggested that the recognition of inflammatory responses and the ability to initiate immune responses were suppressed after the PCV2 infection. In summary, the PCV2 infection inhibited the immune function of the ileal mucosa.

The expression of the genes related to the defense responses, inflammatory responses, the complement and coagulation cascade reactions, Toll-like receptor responses, and cytokine responses were changed at the effector site. Eighteen differentially expressed genes were involved (12 were upregulated, and 6 were downregulated) (**Table 3**). The expression levels of the genes related to the inflammatory responses, *IL-1α*, *IL-1β*, and *IL-6*, were upregulated significantly. The expression levels of genes related to the Toll-like receptor and cytokine responses, *CD40*, *CD80*, *CCL5*, *CXCL10*, *CXCL9*, *IL-6*, and *IL-1β* were also upregulated remarkably. The results suggest that the inflammatory reactions and innate immune responses at the effector site were enhanced after the PCV2 infection. On the other hand, the expression levels of the genes related to the complement reactions, *C3* and *C5*, as well as the genes related to defense responses, *SAA2* and *CCL4*, were downregulated significantly. The expression of *IFNε* was also downregulated remarkably. All the results above indicated that although the innate immune response was enhanced to some degree, the antiviral capacity was suppressed at the effector site.

Table 2. Gene ontology functional classification of genes that are differentially expressed at the induction site

Item	No.	Gene
Complement and coagulation cascades	7	↓: C1QA. C5. C6. C8A. C9. CFH. F5
Inflammatory response	6	↑: IL-1B
		↓: C1QA. CCL25. C5. SAA2. CD163
Defense response	7	↑: IL-1β
		↓: C1QA. CCL25. IFNE. C5. SAA2. CD163
Intestinal immune network for IgA production	4	↓: SLA-DRB1. CCL25. CCL28. PIGR

IgA, immunoglobulin A.
p < 0.05 compared to uninfected sample of piglet.

Table 3. Gene ontology functional classification of genes that are differentially expressed at the effector site

Item	No.	Gene
Inflammatory response	7	↑: CCL4. IL-1A. IL-6. IL-1B. SAA2
		↓: C3. C5
Complement and coagulation cascades	7	↑: THBD. PROC
		↓: C3. C5. C6. C8A. C9
Defense response	8	↑: CCL4. IL1A. IL-6. IL-1B. SAA2
		↓: C3. C5. IFNE
Toll-like receptor signaling pathway	7	↑: CD40. CD80. CCL5. CXCL10. CXCL9. IL-6. IL-1B
Cytokine-cytokine receptor interaction	10	↑: CD40. CCL4. CCL5. CCR3. CXCL10. CXCL9. IL-1A. IL-6. IL-1B
		↓: IFNE

p < 0.05 compared to uninfected sample of piglet.

The total RNA was extracted from the effector and induction sites of the infection and control groups. The expression levels of all genes above were verified by qRT-PCR. All results are consistent with the gene chip results (**Fig. 2**), indicating that the results from the gene chip were reliable.

PCV2 infection enhanced the antigen-processing and presentation abilities of the ileum

Compared to the control group, the ratio of DCs and CD80/86-MHCII$^+$ cells at the effector (mucosal epithelial cells and lamina propria cells) and induction sites increased significantly at 21 dpi in the infection group (**Fig. 3**). This suggests that the PCV2 infection enhanced the antigen-processing and presentation abilities of the ileum.
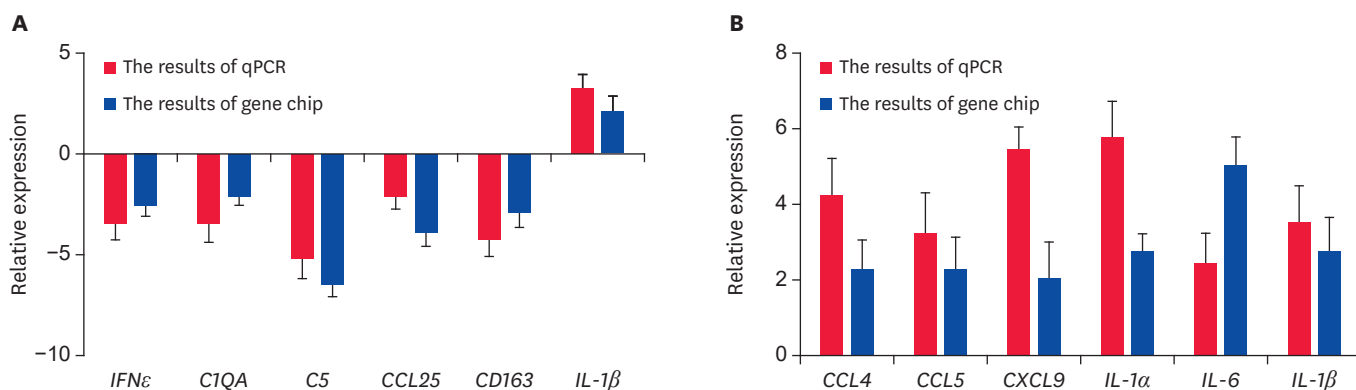
Fig. 2. Gene expression levels at the effector and induction sites. (A) *IFNε*, *C1QA*, *C5*, *CCL25*, *CD163*, and *IL-1β* mRNA expression at the induction site after a PCV2 infection. (B) *CCL4*, *CCL5*, *CXCL9*, *IL-1α*, *IL-6*, and *IL-1β* mRNA expression at the effector site after a PCV2 infection. In (A) and (B), the relative expression levels were measured by gene chip and verified by qRT-PCR (n = 3 per group). Error bars represent standard deviations.
qPCR, quantitative polymerase chain reaction; mRNA, messenger RNA; PCV2, porcine circovirus type 2; qRT-PCR, quantitative reverse transcription-polymerase chain reaction.
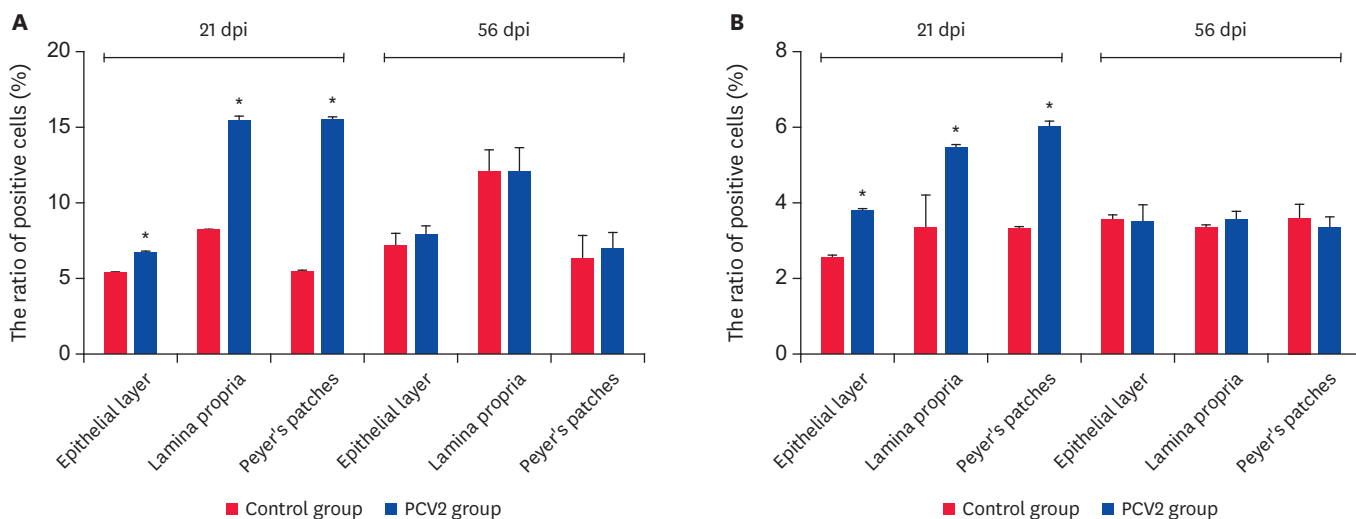
Fig. 3. Ratio of DCs and CD80/86-MHCII$^+$ cells in the epithelial layer, lamina propria and Peyer's patches at 2 time points. (A) Ratio of DCs. (B) Ratio of CD80/86-MHCII$^+$ cells. The values represent the positive cell rate (%) (n = 3 per group). One hundred percent represents all cells in this experiment. The error bars represent the SDs.
PCV2, porcine circovirus type 2; dpi, days post-infection; DC, dendritic cell.
*p < 0.05.
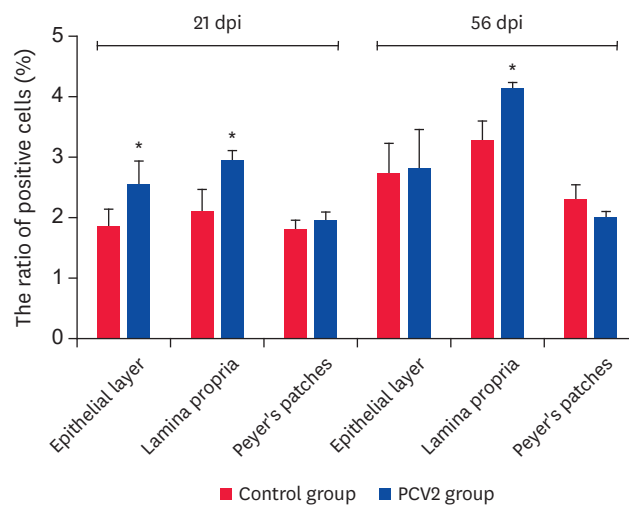
Fig. 4. Ratio of B lymphocytes in various regions of the ileum. The ratio of B lymphocytes in the epithelial layer, lamina propria and Peyer's patches at 2 time points. Values represent the positive cell rate (%) (n = 3 per group). One hundred percent represents all cells in this experiment. Error bars represent SDs.
PCV2, porcine circovirus type 2; dpi, days post-infection.
*$p < 0.05$.

PCV2 infection is involved in the cellular and humoral immunity of the ileum

The ratio of B lymphocytes was increased significantly at the effector site at 21 dpi and only at the lamina propria of the effector site at 56 dpi ($p < 0.05$) (**Fig. 4**). The ratio of T lymphocytes was increased significantly at the induction site and lamina propria of the effector site at 21 dpi. This only increased significantly at the effector site at 56 dpi ($p < 0.05$) (**Fig. 5A**). The ratio of $CD4^+/CD8$ T cells decreased significantly at the induction site and lamina propria of the effector site at 21 dpi ($p < 0.05$) (**Fig. 5B**). Furthermore, the ratio of $CD4^-/CD8^+$ T cells increased significantly at the induction site and lamina propria of the effector site at 21 dpi ($p < 0.05$). In contrast, it declined significantly at the epithelial layer of the effector site at 21 dpi ($p < 0.05$) (**Fig. 5C**). This indicates that the PCV2 infection was involved in the cellular and humoral immunity of the ileum.

PCV2 infection could enhance lymphocyte proliferation

At 21 dpi, compared to the control group, the lymphocyte proliferative capacity of PCV2-infected group was higher at the induction site and significantly higher at the lamina propria of the effector site ($p < 0.05$). In contrast, it was inhibited at the epithelial layer of the induction site (**Fig. 6**). No significant change was observed at 56 dpi, suggesting that a PCV2 infection could enhance lymphocyte proliferation at the effector site at 21 dpi.

PCV2 infection inhibited SIgA production at a high viral nucleic acid load

Compared to the control group, the SIgA expression level of the PCV2-infected group was downregulated significantly at 21 dpi ($p < 0.05$) (**Fig. 7**). On the other hand, there was no significant change at 56 dpi. This suggests that SIgA expression was inhibited when the viral nucleic acid load was high, while it recovered when the viral nucleic acid load declined.
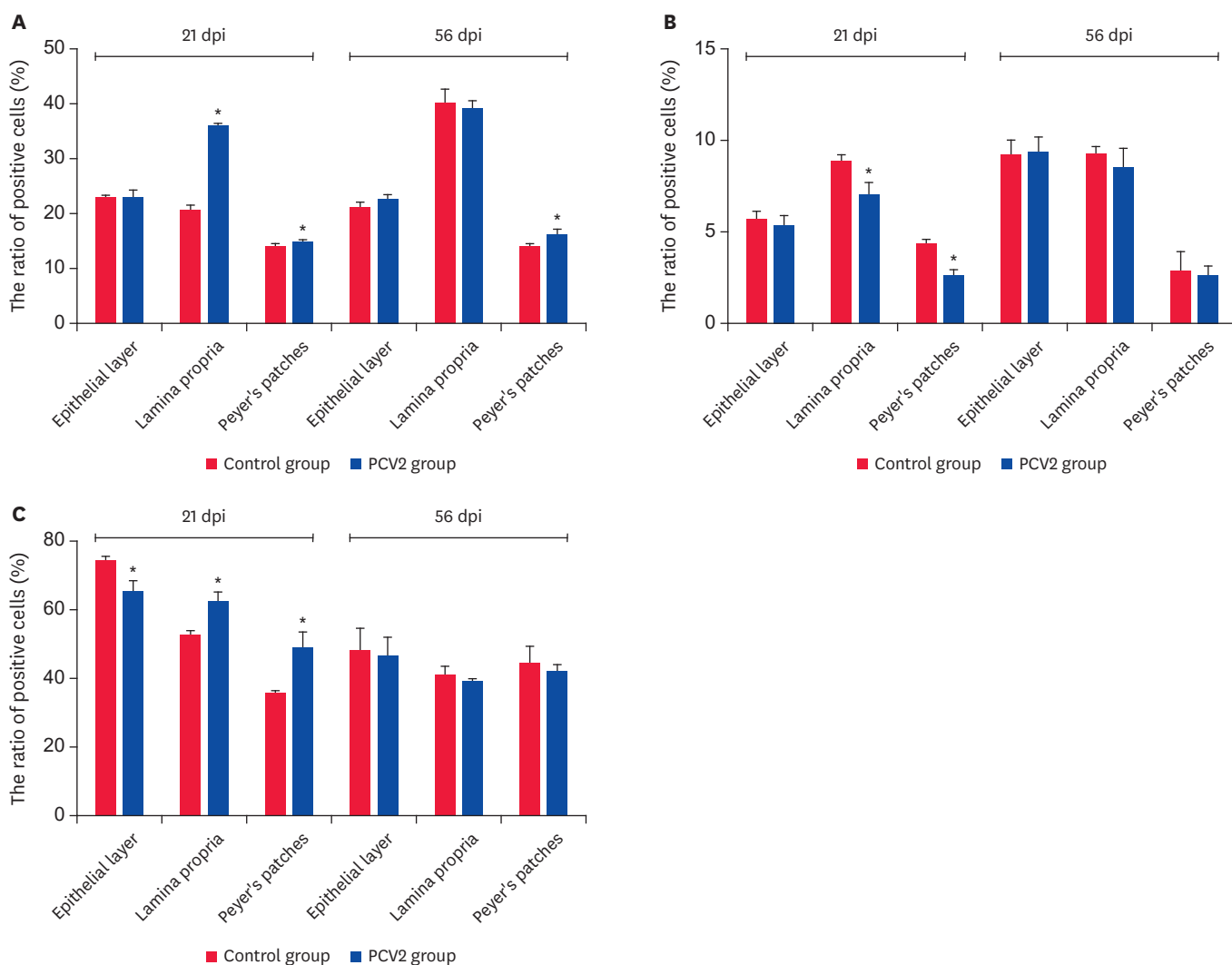
Fig. 5. The ratio of T lymphocytes, CD4$^+$T lymphocytes and CD8$^+$T lymphocytes in the epithelial layer, lamina propria and Peyer's patches at 2 time points. (A) Ratio of total T lymphocytes. (B) Ratio of CD4$^+$T lymphocytes. (C) Ratio of CD8$^+$T lymphocytes. The values represent the positive cell rate (%) (n = 3 per group). One hundred percent represents all cells in this experiment. The error bars represent SDs.
PCV2, porcine circovirus type 2; dpi, days post-infection.
*$p < 0.05$.

DISCUSSION

This study revealed the changes in the immune-related molecules and cells in the ileum of piglets after a PCV2 infection. The morphological changes within the ileum during a PCV2 infection were consistent with the result of a previous report [13]. This indicates that a PCV2 infection caused ileal damage in piglets. In addition, the piglets infected with PCV2 also showed vascular dysfunction [14]. This study showed that the expression of thrombomodulin (*THBD*) and protein C (*PROC*) were upregulated significantly at the effector site. In contrast, the coagulation factor (*F5*) was downregulated significantly at the induction site after the PCV2 infection. *THBD* is a vital coagulation inhibitor because it binds to thrombin to reduce the clotting activity and activates *PROC* to enhance the anticoagulation activity [15]. *F5* is also important to coagulation processes [16]. The results suggest that the blood coagulation
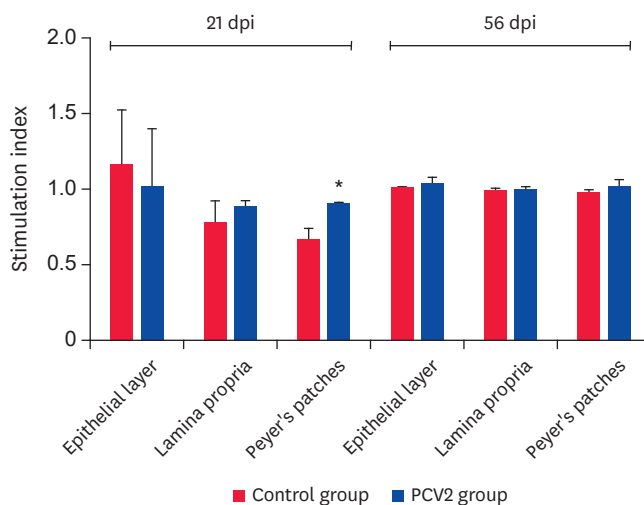
Fig. 6. Proliferation capacity of T lymphocytes in various lymphoid tissues of the ileum. The stimulation index of T lymphocytes was determined using an MTS assay (cell proliferation assay). Error bars represent the SDs.
PCV2, porcine circovirus type 2; dpi, days post-infection.
*$p < 0.05$.
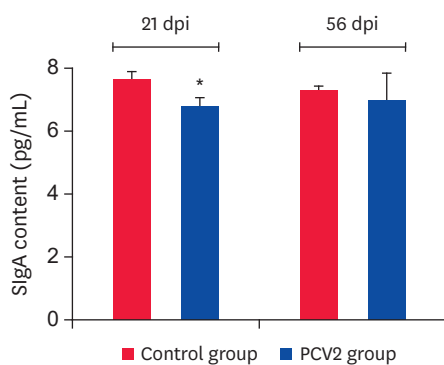
Fig. 7. Content changes in SIgA in the ileum after PCV2 infection. ELISA analysis demonstrated that SIgA protein reacts with a biotinylated anti-SIgA antibody in the PCV2 group. The uninfected group was used as a negative control.
PCV2, porcine circovirus type 2; dpi, days post-infection; SIgA, secretory immunoglobulin A.
*$p < 0.05$.

function of the ileum was suppressed to some degree after PCV2 infection. This may explain the reason for vascular dysfunction and villus exfoliation of the ileum after a PCV2 infection.

The complement acts as an inflammatory mediator and helps lyse the target cells and promote the ability of virus phagocytosis and neutralization [17]. In this study, the complement-related molecules were downregulated significantly at the induction and effector sites after the PCV2 infection. This suggests that a PCV2 infection could inhibit the function of the complement system in the ileum. The virus phagocytosis and neutralization ability of ileum could be suppressed to some degree after inhibition of the complement system, which is beneficial to virus survival *in vivo*. This result may explain the reason for the ileal immune function inhibition and PCV2 continuous survival *in vivo*.

The PCV2-infected piglets showed post-weaning multisystemic wasting syndrome, which manifests as a significant increase in proinflammatory cytokines (*IL-1α*, *IL-1β*, and *IL-6*) *in vivo* [18]. The results showed that the levels of *IL-1α*, *IL-1β*, and *IL-6* expression were upregulated

significantly after the PCV2 infection. Moreover, the PCV2 infection contributed to the ileal inflammation. In addition, the expression of *SAA2* (an indicator of inflammation) [19] and *CD163* (a molecule that can interact with hemoglobin-binding globin complexes to play a role in anti-inflammatory and antioxidant processes [20]) were also upregulated, indicating the presence of an anti-inflammatory response. *CCL4* and *CCL5* contribute to the inflammation response by regulating the function of the T cells, NK cells, monocytes, and immature DCs [21]. The upregulation of *CCL4* and *CCL5* expression at the effector site also indicated that the inflammatory response was activated. All the molecular changes above indicated that a PCV2 infection contributed to the development of ileal inflammation.

DC plays an important role in antigen recognition, antigen presentation, and T cell activation [22]. Intestinal DCs are distributed mainly in the intestinal lamina propria, Peyer's patches, and mesenteric lymph nodes [23]. By ingesting different foreign antigens, the intestinal DCs contribute to SIgA switching and the lymphocytes homing process [24]. The number and subset changes of ileal DCs can affect the antigen presentation capacity of the ileum. These results showed that the ratios of DCs and CD80/86-MHCII+ cells were increased in the ileal mucosa and lymph nodes at 21 dpi, indicating that the antigen presentation capacity of the ileum was enhanced after the PCV2 infection.

B cells are classified into B1 and B2 cells [25]. The B1 cell is a type of antigen-presenting cell, and the B2 cell is involved in humoral immunity with the function of antibody secretion [25]. SIgA, which is formed by the secretory fragments of epithelial cells combined with multimeric IgA, is secreted by plasma cells (B2 cells) into the exocrine fluid via polymeric Ig receptor (*PIGR*) transportation [26,27]. This is the first line to protect the intestinal epithelial cells against pathogenic microorganisms and toxins [26]. *CCL28* can also induce the extensive mucosal migration of IgA+ antibody-secreting cells [28]. The result showed that the expression of *PIGR* and *CCL28* were both downregulated after the PCV2 infection. Although the ratio of B cells was increased significantly at the effector site at 21 dpi, the SIgA content was decreased significantly. This might be because the downregulations of *PIGR* and *CCL28* expression inhibited the synthesis, migration, and secretion of SIgA, which weakened the ileal humoral immunity capacity of the infected piglets. The SIgA content is also beneficial to the virus survival *in vivo*. The precise mechanism of this phenomenon should be clarified.

Pathogen-activated CD8+T cells can secrete cytokines to induce cytotoxic effects and exacerbate enteritis [29,30]. *CXCL9* and *CXCL10* can recruit T cells to the peripheral inflammation site [31]. In the lamina propria and Peyer's patches at 21 dpi, the expression of some chemokines (*CXCL9* and *CXCL10*) was upregulated; the ratio of CD4+T cells was decreased; the ratio of CD8+T cells was increased, and the proliferation capacity of T cells was enhanced, indicating that the cytotoxic effects were enhanced in the ileum. The results suggested that more CD8+T cells migrated to the inflammatory site of the ileum after the PCV2 infection, which aggravated enteritis. This may also be a critical mechanism of PCV2-induced enteritis that requires further study.

Therefore, a PCV2 infection could cause ileal damage to piglets and change immune-related genetic expression, immune cell subsets, and SIgA production of the ileum. These results showed that the molecular changes were induced by PCV2 within the ileal mucosa of the piglets, which would help understand the pathogenesis of PCV2 and might provide a basis for a further study of PCV2-induced enteritis.

SUPPLEMENTARY MATERIALS

Supplementary Fig. 1

Viremia of PCV2 infected piglets. The piglets of the infection group were inoculated with PCV2 at $10^{5.25}$ TCID$_{50}$/mL. Serum were harvested at 3, 7, 14, 21, 28, 35, 42, 49, and 56 dpi. The viral DNAs were quantitated by qPCR assay. The values are the means ± SEM for 3 samples.

Click here to view

Supplementary Fig. 2

Electrophoretic result of PCV2-amplified products from the ileum of the infected and uninfected piglets. DNA fragment of PCV2 was amplified by PCR. Lane M, DNA marker (100 bp Ladder Marker; TransGen Biotech, China). Lane 1–3, the result of the infection group at 21 dpi (one piglet sample each Line). Lane 4–6, the result of the infection group at 56 dpi (one piglet sample each Line). Lane 7–9, result of the control group at 21 dpi (one piglet sample each Line). Lane 10–12, result of the control group at 56 dpi (one piglet sample each Line). The primers of PCV2 for PCR were listed in **Table 1**.

Click here to view

REFERENCES

1. Allan GM, Ellis JA. Porcine circoviruses: a review. J Vet Diagn Invest. 2000;12(1):3-14.
   PUBMED | **CROSSREF**
2. Kim J, Ha Y, Jung K, Choi C, Chae C. Enteritis associated with porcine circovirus 2 in pigs. Can J Vet Res 2004;68(3):218-221.
   PUBMED
3. Opriessnig T, Madson DM, Roof M, Layton SM, Ramamoorthy S, Meng XJ, et al. Experimental reproduction of porcine circovirus type 2 (PCV2)-associated enteritis in pigs infected with PCV2 alone or concurrently with *Lawsonia intracellularis* or *Salmonella typhimurium*. J Comp Pathol. 2011;145(2-3):261-270.
   PUBMED | **CROSSREF**
4. Allan GM, Kennedy S, McNeilly F, Foster JC, Ellis JA, Krakowka SJ, et al. Experimental reproduction of severe wasting disease by co-infection of pigs with porcine circovirus and porcine parvovirus. J Comp Pathol. 1999;121(1):1-11.
   PUBMED | **CROSSREF**
5. Opriessnig T, Halbur PG. Concurrent infections are important for expression of porcine circovirus associated disease. Virus Res. 2012;164(1-2):20-32.
   PUBMED | **CROSSREF**
6. Chae C. A review of porcine circovirus 2-associated syndromes and diseases. Vet J. 2005;169(3):326-336.
   PUBMED | **CROSSREF**
7. Wittig BM, Zeitz M. The gut as an organ of immunology. Int J Colorectal Dis. 2003;18(3):181-187.
   PUBMED | **CROSSREF**
8. Macdonald TT, Monteleone G. Immunity, inflammation, and allergy in the gut. Science. 2005;307(5717):1920-1925.
   PUBMED | **CROSSREF**
9. Ventura M, Turroni F, Motherway MO, MacSharry J, van Sinderen D. Host-microbe interactions that facilitate gut colonization by commensal bifidobacteria. Trends Microbiol. 2012;20(10):467-476.
   PUBMED | **CROSSREF**
10. Jung C, Hugot JP, Barreau F. Peyer's patches: the immune sensors of the intestine. Int J Inflamm. 2010;2010:823710.
    PUBMED | **CROSSREF**

11. Lefrançois L, Lycke N. Isolation of mouse small intestinal intraepithelial lymphocytes, Peyer's patch, and lamina propria cells. Curr Protoc Immunol. 2001;Chapter 3:Unit 3.19.
    PUBMED | CROSSREF

12. Bagheri H, Pourhanifeh MH, Derakhshan M, Mahjoubin-Tehran M, Ghasemi F, Mousavi S, et al. CXCL-10: a new candidate for melanoma therapy? Cell Oncol (Dordr). 2020;43(3):353-365.
    PUBMED | CROSSREF

13. Jung K, Ha Y, Ha SK, Kim J, Choi C, Park HK, et al. Identification of porcine circovirus type 2 in retrospective cases of pigs naturally infected with porcine epidemic diarrhoea virus. Vet J. 2006;171(1):166-168.
    PUBMED | CROSSREF

14. Resendes AR, Segalés J. Characterization of vascular lesions in pigs affected by porcine circovirus type 2-systemic disease. Vet Pathol. 2015;52(3):497-504.
    PUBMED | CROSSREF

15. Takano S, Kimura S, Ohdama S, Aoki N. Plasma thrombomodulin in health and diseases. Blood. 1990;76(10):2024-2029.
    PUBMED | CROSSREF

16. Kanaji S, Kanaji T, Honda M, Nakazato S, Wakayama K, Tabata Y, et al. Identification of four novel mutations in F5 associated with congenital factor V deficiency. Int J Hematol. 2009;89(1):71-75.
    PUBMED | CROSSREF

17. Dunkelberger JR, Song WC. Complement and its role in innate and adaptive immune responses. Cell Res. 2010;20(1):34-50.
    PUBMED | CROSSREF

18. Sipos W, Duvigneau JC, Willheim M, Schilcher F, Hartl RT, Hofbauer G, et al. Systemic cytokine profile in feeder pigs suffering from natural postweaning multisystemic wasting syndrome (PMWS) as determined by semiquantitative RT-PCR and flow cytometric intracellular cytokine detection. Vet Immunol Immunopathol. 2004;99(1-2):63-71.
    PUBMED | CROSSREF

19. Peters SM, Yancy H, Deaver C, Jones YL, Kenyon E, Chiesa OA, et al. In vivo characterization of inflammatory biomarkers in swine and the impact of flunixin meglumine administration. Vet Immunol Immunopathol. 2012;148(3-4):236-242.
    PUBMED | CROSSREF

20. Kristiansen M, Graversen JH, Jacobsen C, Sonne O, Hoffman HJ, Law SK, et al. Identification of the haemoglobin scavenger receptor. Nature. 2001;409(6817):198-201.
    PUBMED | CROSSREF

21. Allen SJ, Crown SE, Handel TM. Chemokine: receptor structure, interactions, and antagonism. Annu Rev Immunol. 2007;25(1):787-820.
    PUBMED | CROSSREF

22. Summerfield A, McCullough KC. The porcine dendritic cell family. Dev Comp Immunol. 2009;33(3):299-309.
    PUBMED | CROSSREF

23. Rescigno M. Intestinal dendritic cells. Adv Immunol. 2010;107:109-138.
    PUBMED | CROSSREF

24. Kelsall B. Recent progress in understanding the phenotype and function of intestinal dendritic cells and macrophages. Mucosal Immunol. 2008;1(6):460-469.
    PUBMED | CROSSREF

25. LeBien TW, Tedder TF. B lymphocytes: how they develop and function. Blood. 2008;112(5):1570-1580.
    PUBMED | CROSSREF

26. Hendrickson BA, Rindisbacher L, Corthesy B, Kendall D, Waltz DA, Neutra MR, et al. Lack of association of secretory component with IgA in J chain-deficient mice. J Immunol 1996;157(2):750-754.
    PUBMED

27. Johansen FE, Braathen R, Brandtzaeg P. Role of J chain in secretory immunoglobulin formation. Scand J Immunol. 2000;52(3):240-248.
    PUBMED | CROSSREF

28. Lazarus NH, Kunkel EJ, Johnston B, Wilson E, Youngman KR, Butcher EC. A common mucosal chemokine (mucosae-associated epithelial chemokine/CCL28) selectively attracts IgA plasmablasts. J Immunol. 2003;170(7):3799-3805.
    PUBMED | CROSSREF

29. Gallimore A, Glithero A, Godkin A, Tissot AC, Plückthun A, Elliott T, et al. Induction and exhaustion of lymphocytic choriomeningitis virus-specific cytotoxic T lymphocytes visualized using soluble tetrameric major histocompatibility complex class I-peptide complexes. J Exp Med. 1998;187(9):1383-1393.
    PUBMED | CROSSREF

30. Müller S, Lory J, Corazza N, Griffiths GM, Z'graggen K, Mazzucchelli L, et al. Activated CD4+ and CD8+ cytotoxic cells are present in increased numbers in the intestinal mucosa from patients with active inflammatory bowel disease. Am J Pathol 1998;152(1):261-268.
   PUBMED

31. Jin T, Xu X, Hereld D. Chemotaxis, chemokine receptors and human disease. Cytokine. 2008;44(1):1-8.
   PUBMED | CROSSREF